THE UNIVERSITY of EDINBURGH

Edinburgh Research Explorer

Europium-IV: An Incommensurately Modulated Crystal Structure in the Lanthanides

Citation for published version:
Husband, R, Loa, I, Stinton, G, Evans, S, Ackland, G & Mcmahon, M 2012, 'Europium-IV: An Incommensurately Modulated Crystal Structure in the Lanthanides', *Physical Review Letters*, vol. 109, no. 9, 095503. https://doi.org/10.1103/PhysRevLett.109.095503

Digital Object Identifier (DOI):
10.1103/PhysRevLett.109.095503

Link:
Link to publication record in Edinburgh Research Explorer

Document Version:
Publisher's PDF, also known as Version of record

Published In:
Physical Review Letters

General rights
Copyright for the publications made accessible via the Edinburgh Research Explorer is retained by the author(s) and / or other copyright owners and it is a condition of accessing these publications that users recognise and abide by the legal requirements associated with these rights.

Take down policy
The University of Edinburgh has made every reasonable effort to ensure that Edinburgh Research Explorer content complies with UK legislation. If you believe that the public display of this file breaches copyright please contact openaccess@ed.ac.uk providing details, and we will remove access to the work immediately and investigate your claim.

Download date: 06. May. 2023

Europium-IV: An Incommensurately Modulated Crystal Structure in the Lanthanides

R. J. Husband,[1] I. Loa,[1] G. W. Stinton,[1] S. R. Evans,[2,*] G. J. Ackland,[1] and M. I. McMahon[1]

[1]*SUPA, School of Physics and Astronomy and Centre for Science at Extreme Conditions, The University of Edinburgh, Mayfield Road, Edinburgh, EH9 3JZ, United Kingdom*

[2]*European Synchrotron Radiation Facility, 38043 Grenoble, France*

(Received 18 May 2012; published 27 August 2012)

High-resolution x-ray powder-diffraction experiments were performed on europium metal at high pressure up to 50 GPa. At variance with previous reports, the hcp phase of Eu was observed to be stable not only to 18 GPa, but to 31.5 GPa. At 31.5(5) GPa, europium transforms to a phase (Eu-IV) with an incommensurately modulated monoclinic crystal structure with superspace group $C2/c(q_1 0 q_3)00$. This new phase was observed to be stable to ~37.0 GPa, where another phase transition was observed. Eu-IV is the first phase in the lanthanide elements with an incommensurate crystal structure.

DOI: 10.1103/PhysRevLett.109.095503 PACS numbers: 61.50.Ks, 62.50.−p, 64.70.Rh

Because of its half-filled $4f^7$ electron shell, europium is a divalent metal at ordinary conditions and, therefore, unlike the majority of the lanthanide elements, which are trivalent. As a result, Eu has a significantly larger atomic volume at ambient pressure, and a larger compressibility, than the neighboring lanthanides [1,2], and the high-pressure phase transitions of Eu are also different from those observed in the trivalent lanthanides [1–3].

In the x-ray diffraction study by Takemura and Syassen [2], Eu was observed to transform from its ambient-pressure body-centered cubic (bcc) phase to hexagonal close-packed (hcp) near 12.5 GPa, a transition that also occurs in divalent barium [4]. At pressures exceeding 18 GPa, the same authors observed the appearance of several diffraction lines in addition to those from the hcp phase. This was attributed to a transition to a new phase, Eu-III, with a structure thought to be closely related to hcp, possibly based on a large supercell. The additional weak reflections were also observed in a subsequent study by Krüger *et al.* [5], who reported further changes in the diffraction patterns of Eu above 32 GPa, but little effort was made over the following two decades to determine the crystal structures of Eu at high pressure.

Interest in the high-pressure behavior of Eu has been rekindled only very recently by the discovery of superconductivity in Eu above 80 GPa, with a critical temperature of $T_c \approx 1.8$ K [6]. In an x-ray diffraction study to 92 GPa, supported by *ab initio* structure prediction calculations, Bi *et al.* [7] confirmed the appearance of additional reflections above 18 GPa and concluded that two regions of phase mixture exist from 18 to 66 GPa: A mixture of hcp and a monoclinic phase from 18 to ~35 GPa and a mixture of the same monoclinic phase and an orthorhombic phase from ~35 to 66 GPa. The phase with the orthorhombic crystal structure was reported to be stable up to at least 92 GPa.

However, we have recently shown that the changes at ~18 GPa are in fact due to the appearance of diffraction peaks from a rhombohedral contaminant phase, and not due to a transition in Eu itself [8]. This raises concerns about the above structure assignments, and leaves us in a situation, where—50 years after the first high-pressure studies on Eu—we are lacking a basic understanding of the crystal structures of this element at pressures as low as 35 GPa. In view of this, we have made an effort to obtain contaminant-free samples of Eu at high pressure and to perform powder x-ray diffraction experiments with very high angular resolution up to a pressure of 50 GPa. We confirm that there is no phase transition in Eu at 18 GPa, and that Eu remains in the hcp phase up to ~31.5 GPa, at which point it transforms to a phase (Eu-IV) with a complex, incommensurately modulated monoclinic crystal structure. This structure is unique among all of the elemental modulated high-pressure structures in that it has a two-dimensional modulation, and it is the first incommensurate structure to be observed in the lanthanide elements.

High-purity Eu samples, supplied by U. Schwarz at the Max-Planck-Institut für Chemische Physik fester Stoffe in Dresden, were loaded into diamond-anvil pressure cells equipped with rhenium gaskets in a dry argon atmosphere (< 0.1 ppm O_2 and < 0.1 ppm H_2O). Due to the history of contamination issues, and because we had observed Eu to discolor even in the argon atmosphere of well-maintained glove boxes, we loaded Eu samples without a pressure-transmitting medium and without a pressure marker, in order to minimize the chances of contamination. The pressure was determined from the position of one or two sample Bragg reflections, using a calibration obtained from high-pressure diffraction experiments on two samples that were loaded with helium as a pressure-transmitting medium and where the pressure was determined with the standard ruby fluorescence method [9].

Angle-dispersive x-ray powder diffraction data were collected on station ID09a at the European Synchrotron Radiation Facility (ESRF), Grenoble, using a beam of monochromatic x rays of wavelength 0.4161 Å collimated

 © 2012 American Physical Society

to a diameter of 15 μm. The data were collected using a mar555 area detector placed either 300 mm, or, in order to improve the angular resolution of the very complex diffraction patterns, 510 mm from the sample. Additional experiments were performed on beam line I15 of the Diamond Light Source, UK, using an x-ray wavelength of 0.338 Å and a mar345 image plate detector. The diffraction patterns were integrated using Fit2D [10,11] and analyzed using the Rietveld method with the JANA2006 software [12]. Once the Eu-IV structure was solved, we were also able to fit the numerous diffraction patterns collected from over 10 different samples both at the ESRF and at the former Synchrotron Radiation Source (SRS), Daresbury—including those where helium was used as a pressure transmitting medium (but all of these samples showed additional contaminant peaks [8]).

We observed the bcc–hcp transition in Eu at 12.5 GPa on pressure increase, in excellent agreement with previous studies [2,5,7]. On further pressure increase, no transition was observed at 18 GPa. Rather, Eu remained in the hcp phase up to a pressure of 31.5 GPa, above which significant changes in the diffraction profiles were observed. This is illustrated in Fig. 1(a), which shows the diffraction patterns of Eu at 30.6 GPa in the hcp phase and at 33.9 GPa after the transition. Note that, unlike in previous studies, the 30.6-GPa pattern comprises only peaks from the hcp phase, and no other. The transition to the new phase, Eu-IV, has been observed in all of our samples that were compressed to above 31.5 GPa.

Two distinct changes were observed in the diffraction patterns at the transition from hcp to Eu-IV. Firstly, our high-resolution data enabled us to observe the splitting of many of the hcp reflections into doublets or triplets, which were not resolved in previous studies. In particular, the intense hcp (101) reflection splits into a triplet, as shown in Fig. 1(d). Secondly, we observed the appearance of more than 30 additional weak reflections, as illustrated in Fig. 1(b).

The splitting of the hcp reflections suggests a transition to a distorted-hcp structure. We first considered the crystal structure with space group *Pnma* (*oP*4 in the Pearson notation) proposed by Bi *et al.* for pressures above 35 GPa [7], as this corresponds to an orthorhombic distortion of the hcp structure. However, we found the overall fit to the split-hcp peaks to be poor. Crucially, the *oP*4 structure does not account for the splitting of the hcp (101) reflection into a triplet. It also cannot account for the large number of weak reflections that appear at 31.5 GPa.

However, an excellent description of the split-hcp reflections was obtained with a monoclinic unit cell. Analysis of the systematic absences showed that all the split-hcp reflections could be indexed based on a structure with space group $C2/c$ and 4 atoms per unit cell (denoted *mC*4 in the Pearson notation) with the atoms in the 4*e* positions at $(0, y, \frac{1}{4})$. At 33.9 GPa, a Rietveld refinement gives lattice parameters of $a = 3.0838(5)$ Å, $b = 5.3002(7)$ Å, $c = 4.7239(4)$ Å, and

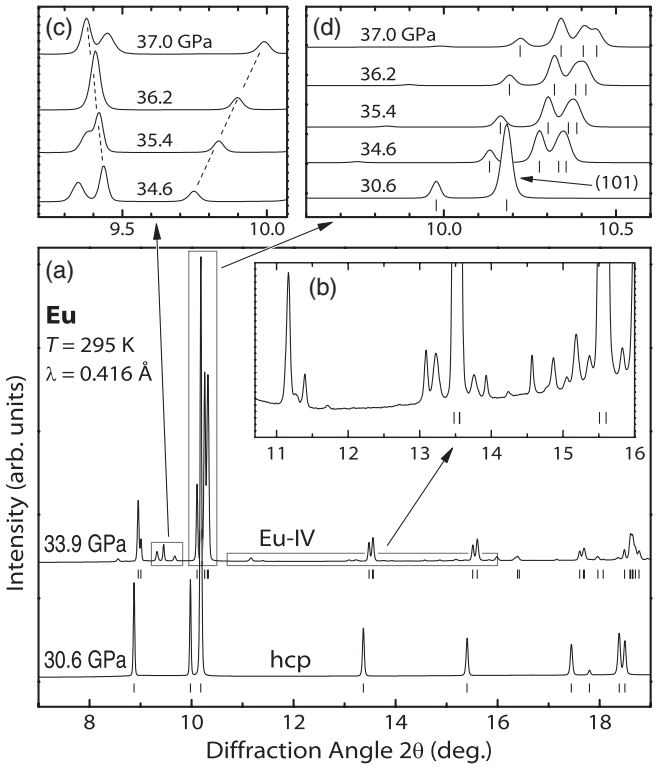

FIG. 1. X-ray powder diffraction patterns of Eu at the transition from hcp to Eu-IV. (a) Diffraction profiles of Eu in the hcp phase at 30.6 GPa and at 33.9 GPa after the transition to Eu-IV. Tick marks indicate the calculated peak positions for the hcp structure (30.6 GPa) and the *mC*4 structure (33.9 GPa). (b) A large number of weak reflections appears at the transition, which the unmodulated *mC*4 structure does not account for. (c) Movement of one of the weak reflections to lower angles (larger *d*-spacings) with increasing pressure. (d) Splitting of the hcp (101) reflection into a triplet, which originates from the monoclinic distortion, as shown by the *mC*4 tick marks.

$\beta = 90.39(1)°$, and the atomic coordinate $y = 0.341(2)$. This represents a small distortion of the hcp structure in the orthohexagonal description, where $b/a = \sqrt{3}$, $\beta = 90°$, and $y = 1/3$.

In Fig. 1, the positions of the *mC*4 reflections are shown by tick marks for the patterns recorded at $P > 31.5$ GPa. It is clear from Fig. 1(d) that the *mC*4 structure correctly accounts for the triplet splitting of the hcp (101) reflection highlighted above. However, it must be stressed that although this structure can account for all the split-hcp reflections, it does not explain any of the additional weak reflections [Fig. 1(b)].

Our attempts to index these weak peaks as a separate phase were unsuccessful. We therefore considered the possibility of indexing them using a superlattice of the *mC*4 structure. We noticed, however, that several of the weak additional reflections move to *lower* angles (longer *d*-spacings) with increasing pressure, whereas all of the split-hcp peaks move to higher angles (smaller *d*-spacings). One such peak is

illustrated in Fig. 1(c). This, combined with the absence of low-angle reflections that would be expected for a larger unit cell, suggested that the many weak additional peaks did not arise from a superstructure of the $mC4$ structure.

We then considered the possibility of an incommensurate structure, with the weak peaks being satellite reflections. The program SUPERCELL [13] was used to index the weak peaks, and we found them to be satellite reflections corresponding to a 2-dimensional modulation vector $\mathbf{q} = (q_1, 0, q_3)$, with $q_1 \approx 0.8$ and $q_3 \approx 0.6$. The resulting superspace group is $C2/c(q_1 0 q_3)00$ (i-$mC4$ in the Pearson notation, where 'i' indicates that the structure is incommensurate).

All of the Bragg peaks observed in the diffraction patterns from Eu above 31.5 GPa can be indexed using four Miller indices, $(hklm)$, according to $\mathbf{H} = h\mathbf{a}^* + k\mathbf{b}^* + l\mathbf{c}^* + m\mathbf{q}$, where $\mathbf{a}^*$, $\mathbf{b}^*$, $\mathbf{c}^*$ define the reciprocal lattice of the $mC4$ structure and $\mathbf{q}$ is the modulation vector. Only first-order ($m = \pm 1$) satellite reflections have been observed. The displacement of an atom in the modulated structure from its average position is given by the modulation function $\mathbf{u}(\bar{x}_4)$, where $\bar{x}_4 = \mathbf{q} \cdot \mathbf{r}_0$ is the fourth superspace component and $\mathbf{r}_0$ is the position of the atom in the average (unmodulated) crystal structure [14]. Taking into account the superspace group symmetry [12], and retaining only the first-order Fourier components, the modulation function for Eu-IV is then given by $\mathbf{u}(\bar{x}_4) = B_{1a}\sin(2\pi\bar{x}_4)\mathbf{a} + A_{1b}\cos(2\pi\bar{x}_4)\mathbf{b} + B_{1c}\sin(2\pi\bar{x}_4)\mathbf{c}$.

Figure 2 illustrates that a Rietveld refinement using the i-$mC4$ structure gives an excellent fit to the diffraction pattern from Eu at 33.9 GPa, with residuals of $R_p = 2.5\%$ and $R_{wp} = 4.2\%$. The satellite reflections account for all of the large number of weak peaks that appear at 31.5 GPa, as illustrated in panel (c), including those that move to lower angles with increasing pressure, such as the $(002\bar{1})$ reflection shown in panel (b). The refined structure at 33.9 GPa is given by $a = 3.0835(1)$ Å, $b = 5.2994(2)$ Å, $c = 4.7239(1)$ Å, $\beta = 90.400(2)$ Å, and $y = 0.342(1)$, with a modulation vector $\mathbf{q} = (0.8095(2), 0, 0.5908(2))$ and modulation amplitudes of $B_{1a} = -0.034(2)$, $A_{1b} = 0.016(1)$, and $B_{1c} = 0.040(1)$.

The i-$mC4$ structure of Eu-IV is the first incommensurately modulated crystal structure observed in the elements at high pressure in which the modulation vector is not in the direction of one of the lattice vectors. Figure 3 shows the unmodulated $mC4$ and the modulated i-$mC4$ structures in comparison. The very close relation to the hcp structure can clearly be seen in the views down the crystallographic c axis in Figs. 3(a) and 3(b).

The i-$mC4$ structure provides an excellent fit to all patterns observed for Eu between 31.5 and 37 GPa. The pressure dependences of the lattice parameters, modulation wave vector and modulation amplitudes are given in the Supplemental Material [15]. In essence, both q_1 and q_3 were observed to decrease with increasing pressure

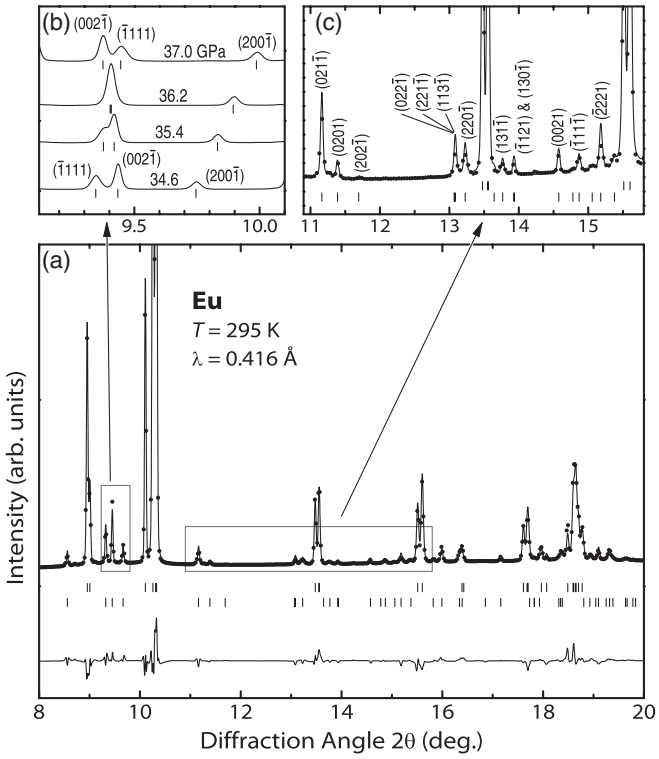

FIG. 2. (a) Rietveld refinement of the Eu i-$mC4$ structure at 33.9 GPa. The symbols show the experimental data and the solid line shows the fit. The upper and lower tick marks show the positions of the main and satellite peaks, respectively, and the residuals are given below the tick marks. Inset (c) illustrates the excellent fit to the large number of weak peaks observed above 31.5 GPa. (b) Movement of the $(002\bar{1})$ reflection to lower angles (larger d-spacing) with increasing pressure.

between 32.4 and 37.0 GPa, and q_1 passes smoothly through $q_1 = 0.8 = 4/5$, which corresponds to a commensurate modulation in this direction. The modulation amplitudes ($|B_{1a}|$, A_{1b}, and B_{1c}) were all found to increase with increasing pressure. In particular, B_{1c} increases from 0.034(3) to 0.055(8) over the 32.4–37.0 GPa pressure range. The increase in the modulation amplitudes entails an increase in the maximum atomic displacements, and as a consequence, the closest-contact distance in the i-$mC4$ structure decreases more rapidly with increasing pressure than it would in the hcp and the unmodulated $mC4$ structure [15]. Overall, this behavior is reminiscent of that of the incommensurately-modulated high-pressure phase phosphorus-IV [16] and different from that of incommensurately-modulated tellurium-III, where the closest-contact distances remain remarkably constant with increasing pressure [17].

We would like to note that Krüger *et al.* [5] reported the appearance of additional peaks in the diffraction patterns of Eu above 32 GPa, and it appears likely that these were evidence of the phase transition to the incommensurate phase. The extra reflections observed in that study are in the correct positions to be the most intense satellite

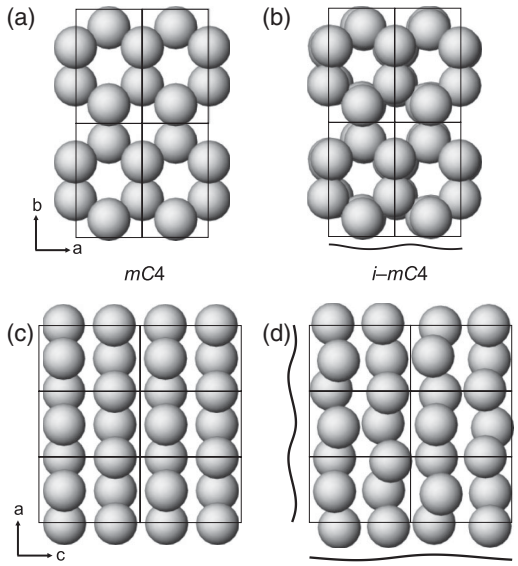

FIG. 3. Schematic views of the hypothetical $mC4$ and the experimentally observed i-$mC4$ crystal structures at 33.9 GPa. Four unit cells viewed along the c direction of (a) unmodulated $mC4$ and of (b) modulated i-$mC4$. Six unit cells viewed along the b direction of (c) unmodulated $mC4$ and of (d) modulated i-$mC4$. Projections of the modulation function $\mathbf{u}(\bar{x}_4)$ onto the ab and ac planes, evaluated along the crystallographic axes, are shown besides the crystal structures in (b) and (d), respectively. The modulation function along the b axis is 0 and therefore not shown.

reflections of Eu-IV, but the limited resolution in this energy-dispersive x-ray diffraction study made it impossible to resolve the splitting of the hcp reflections and other details. Bundy and Dunn observed a step in the electrical resistance of Eu near 28 GPa at room temperature [18], and this may also be related to the transition from hcp to the i-$mC4$ phase at 31.5 GPa.

Upon compression to above 37.0 GPa, we observed further changes in the diffraction profiles of Eu that indicate a transition to another new phase. The complexity of the diffraction patterns suggests that this phase may also have a modulated crystal structure, but this remains to be determined in detail.

It is highly desirable to identify the mechanism that leads to the formation of the incommensurate modulation in Eu-IV, presumably via strong electron-phonon coupling or extreme Kohn anomalies, but europium is well known to be among the elements that are the most difficult to treat in electronic structure calculations in the framework of density functional theory (DFT). The challenge is to describe the properties of the half-filled shell of relatively localized $4f$ electrons accurately. Treating the $4f$ states as regular valence states in the local density approximation leads to a significant overbinding: The calculated equilibrium volume is too small by 15% and 33% in the spin-polarized and the nonpolarized case, respectively, which is far more than the few percent typical in DFT calculations [19].

In a recent computational search for the crystal structures of Eu metal at high pressure [7], the $4f$ electrons were treated as core states, and the projector-augmented wave (PAW) method [20] was used together with the generalized gradient approximation (GGA); this reduced the underestimation of the equilibrium volume to slightly less than 10% for both the spin-polarized and the nonpolarized case. We used the same approach (as implemented in the ABINIT code [21]) in an initial attempt to identify the origin of both the monoclinic distortion and the incommensurate modulation, but found the variation of the calculated axial ratio in the hcp phase, c/a, to be inconsistent with the experimental results (see the Supplemental Material [15] for details). For example, these calculations yielded $c/a = 1.34$ at 20 GPa, which is much smaller than the experimental value of 1.56. Treating the $4f$ states as core states is therefore not an adequate approximation for modeling the properties of Eu metal at high pressure.

To test an alternative approach, we have also performed spin-polarized calculations in the generalized gradient approximation with additional treatment of on-site Coulomb repulsion for the $4f$ states, using the DFT + U scheme [22] as implemented in the "full-potential augmented plane-wave plus local orbital" code, WIEN2K [15,23]. This yielded a calculated equilibrium volume in good agreement with the experiment, i.e., 3% larger than the experimental value, which is typical for GGA-based DFT calculations. In addition, the calculated decrease in c/a with increasing pressure leveled off at 1.55, which is also in good agreement with the experiment. However, the calculation yields the rapid reduction in c/a only at a higher pressure (by $\sim$13 GPa) than observed experimentally. Overall, a better description of Eu at high pressure is obtained with the DFT + U approach than by treating the $4f$ states as core states, but there is clearly a need for further improvement.

In future computational work, the possible pressure-dependence of the effective on-site Coulomb repulsion [24] should be considered, but it may prove necessary to go beyond the DFT + U scheme, with dynamical mean field theory (DMFT) being a possible alternative [25]. The accurate modeling of the electronic structure of Eu at high pressure remains a great challenge, and the present detailed experimental results on the structural evolution of Eu metal under pressure provide stringent tests for future work in this direction.

In summary, we have determined that Eu-IV, which is stable from 31.5 to 37 GPa, has an incommensurately modulated crystal structure, the first of this type to be observed in a lanthanide element. Eu-IV is also the first high-pressure incommensurate elemental structure in which the modulation vector is not in the direction of one of the crystallographic axes. Eu is well known to be challenging for DFT calculations. These experimental observations warrant new, dedicated electronic structure calculations aimed

at uncovering the mechanism that leads to Eu's unusual high-pressure behavior.

This work was supported by grants and a fellowship (I. L.) from the UK Engineering and Physical Sciences Research Council, and facilities were made available by the European Synchrotron Radiation Facility, Diamond Light Source, and SRS Daresbury. We thank L. F. Lundegaard and O. Degtyareva for their help with the experiments in the early stage of this study, U. Schwarz for providing Eu samples, and M. Hanfland, A. Lennie, and N. Casati for their support on the beam lines.

*Present address: Departement für Chemie und Biochemie, Universität Bern, Switzerland and Swiss Light Source, PSI, Villigen, Switzerland.

[1] B. Johansson and A. Rosengren, Phys. Rev. B **11**, 2836 (1975).
[2] K. Takemura and K. Syassen, J. Phys. F **15**, 543 (1985).
[3] A. Jayaraman and R. Sherwood, Phys. Rev. **134**, A691 (1964).
[4] J. D. Barnett, R. B. Bennion, and H. T. Hall, Science **141**, 534 (1963).
[5] T. Krüger, B. Merkau, W. A. Grosshans, and W. B. Holzapfel, High Press. Res. **2**, 193 (1990).
[6] M. Debessai, T. Matsuoka, J. J. Hamlin, J. S. Schilling, and K. Shimizu, Phys. Rev. Lett. **102**, 197002 (2009).
[7] W. Bi, Y. Meng, R. S. Kumar, A. L. Cornelius, W. W. Tipton, R. G. Hennig, Y. Zhang, C. Chen, and J. S. Schilling, Phys. Rev. B **83**, 104106 (2011).
[8] R. J. Husband, I. Loa, G. W. Stinton, S. R. Evans, G. J. Ackland, and M. I. McMahon, J. Phys. Conf. Ser. **377**, 012030 (2012).
[9] H. K. Mao, J. Xu, and P. M. Bell, J. Geophys. Res. **91**, 4673 (1986).
[10] A. P. Hammersley, computer code FIT2D, 2005.
[11] A. P. Hammersley, S. O. Svensson, M. Hanfland, A. N. Fitch and D. Häusermann, High Press. Res. **14**, 235 (1996).
[12] V. Petrícek, M. Dusek and L. Palatinus, *The Crystallographic Computing System JANA2006* (Institute of Physics, Prague, 2006).
[13] J. Rodrìguez-Carvajal, Physica (Amsterdam) **192B**, 55 (1993).
[14] S. van Smaalen, *Incommensurate Crystallography* (Oxford University, New York, 2007).
[15] See Supplemental Material at http://link.aps.org/supplemental/10.1103/PhysRevLett.109.095503 for details.
[16] H. Fujihisa, Y. Akahama, H. Kawamura, Y. Ohishi, Y. Gotoh, H. Yamawaki, M. Sakashita, S. Takeya, and K. Honda, Phys. Rev. Lett. **98**, 175501 (2007)
[17] C. Hejny and M. I. McMahon, Phys. Rev. Lett. **91**, 215502 (2003).
[18] F. P. Bundy and K. J. Dunn, Phys. Rev. B **24**, 4136 (1981).
[19] B. Min, H. Jansen, T. Oguchi, and A. Freeman, J. Magn. Magn. Mater. **59**, 277 (1986).
[20] P. E. Blöchl, Phys. Rev. B **50**, 17953 (1994).
[21] X. Gonze *et al.*, Comput. Mater. Sci. **25**, 478 (2002), http://www.abinit.org.
[22] V. I. Anisimov, I. V. Solovyev, M. A. Korotin, M. T. Czyżyk, and G. A. Sawatzky, Phys. Rev. B **48**, 16929 (1993).
[23] P. Blaha, K. Schwarz, G. K. H. Madsen, D. Kvasnicka, and J. Luitz, *WIEN2K, An Augmented Plane Wave + Local Orbitals Program for Calculating Crystal Properties* (K. Schwarz, Technische Universität Wien, Vienna, Austria, 2001).
[24] M. Cococcioni and S. de Gironcoli, Phys. Rev. B **71**, 035105 (2005).
[25] A. Georges, G. Kotliar, W. Krauth, and M. J. Rozenberg, Rev. Mod. Phys. **68**, 13 (1996).